

Search for a systematic behavior of the breakup probability in reactions with weakly bound projectiles at energies around the Coulomb barrier

V. V. Sargsyan,^{1,2} G. G. Adamian,¹ N. V. Antonenko,¹ W. Scheid,³ and H. Q. Zhang⁴

¹Joint Institute for Nuclear Research, 141980 Dubna, Russia

²International Center for Advanced Studies, Yerevan State University, 0025 Yerevan, Armenia

³Institut für Theoretische Physik der Justus-Liebig-Universität, D-35392 Giessen, Germany

⁴China Institute of Atomic Energy, Post Office Box 275, Beijing 102413, China

(Received 26 May 2012; revised manuscript received 16 October 2012; published 29 November 2012)

Comparing the capture cross sections calculated without the breakup effect and experimental complete fusion cross sections, the breakup was analyzed in reactions with weakly bound projectiles ${}^6,7,9\text{Li}$, ${}^{9,11}\text{Be}$, and ${}^{6,8}\text{He}$. A trend of systematic behavior for the complete fusion suppression as a function of the target charge and bombarding energy is not achieved. The quasielastic backscattering is suggested as a useful tool to study the behavior of the breakup probability in reactions with weakly bound projectiles.

DOI: [10.1103/PhysRevC.86.054610](https://doi.org/10.1103/PhysRevC.86.054610)

PACS number(s): 25.70.Jj, 24.10.-i, 24.60.-k

I. INTRODUCTION

In recent years, many efforts have been made to understand the effect of the breakup of weakly bound nuclei during fusion in very asymmetric reactions where the capture cross section is equal to the complete fusion cross section [1–9]. The light radioactive nuclei, especially halo nuclei such as ${}^6\text{He}$, ${}^8\text{B}$, and ${}^{11}\text{Be}$, and the stable nuclei ${}^{6,7}\text{Li}$ and ${}^9\text{Be}$ are weakly bounded; hence there is a chance of the breakup in the colliding process. By performing a comparison of fusion data with theoretical predictions, which do not take into account the dynamic breakup plus transfer channel effects, it has been shown [4–6,9] that for energies from about $1.1V_b$ to $1.5V_b$ (V_b is the height of the Coulomb barrier) complete fusion in the reactions ${}^{6,7}\text{Li} + {}^{208}\text{Pb}$, ${}^{209}\text{Bi}$ and ${}^9\text{Be} + {}^{89}\text{Y}$, ${}^{124}\text{Sn}$, ${}^{208}\text{Pb}$, ${}^{209}\text{Bi}$ is suppressed by about 30%. However, the ${}^9\text{Be} + {}^{144}\text{Sm}$ data are out of the systematics, showing a much smaller suppression of about 15%. The total fusion (incomplete fusion + sequential complete fusion + complete fusion) cross section for the same projectiles on targets of any mass, including ${}^9\text{Be} + {}^{27}\text{Al}$, ${}^{64}\text{Zn}$, does not seem to be affected by the dynamic breakup and transfer effects [6,9]. As the charge of the target decreases, one expects that the Coulomb breakup becomes weaker and consequently that the complete fusion suppression and incomplete fusion probability decrease. The lack of a clear systematic behavior of the complete fusion suppression as a function of the target charge was explained in Ref. [9] by different effects of the transfer channels on the complete fusion and by some problems with the experimental data analysis.

In the present article we try to reveal a systematic behavior of the complete fusion suppression as a function of the target charge Z_T and colliding energy $E_{c.m.}$ by using the quantum diffusion approach [10,11] and by comparing the calculated capture cross sections in the absence of breakup with the experimental complete and total fusion cross sections. The effects of deformation and neutron transfer on the complete fusion are taken into consideration.

II. MODEL

In the quantum diffusion approach [10,11] the collision of nuclei is described with a single relevant collective variable: the relative distance between the colliding nuclei. This approach takes into account the fluctuation and dissipation effects in collisions of heavy ions, which model the coupling with various channels (for example, coupling of the relative motion with low-lying collective modes such as dynamical quadrupole and octupole modes of the target and projectile nuclei [12]). We mention that many quantum-mechanical and non-Markovian effects accompanying the passage through the potential barrier are considered in our formalism [10,11,13]. The nuclear deformation effects are taken into account through the dependence of the nucleus-nucleus potential on the deformations and mutual orientations of the colliding nuclei. To calculate the nucleus-nucleus interaction potential $V(R)$, we use the procedure presented in Refs. [10,11]. For the nuclear part of the nucleus-nucleus potential, a double-folding formalism with a Skyrme-type density-dependent effective nucleon-nucleon interaction is used. Within this approach many heavy-ion capture reactions with stable and radioactive beams at energies above and well below the Coulomb barrier have been successfully described [10,11,13]. One should note that other diffusion models that include quantum statistical effects were also proposed in Ref. [14].

We assume that the sub-barrier capture mainly depends on the optimal one-neutron ($Q_{1n} > Q_{2n}$) or two-neutron ($Q_{2n} > Q_{1n}$) transfer with a positive Q value. Our assumption is that just before the projectile is captured by the target nucleus (just before the crossing of the Coulomb barrier), which is a slow process, the transfer occurs that can lead to the population of the first excited collective state in the recipient nucleus [15]. So, the motion to the N/Z equilibrium starts in the system before the capture because it is energetically favorable in the dinuclear system in the vicinity of the Coulomb barrier. For the reactions under consideration, the average change of mass asymmetry is connected to the one- or two-neutron

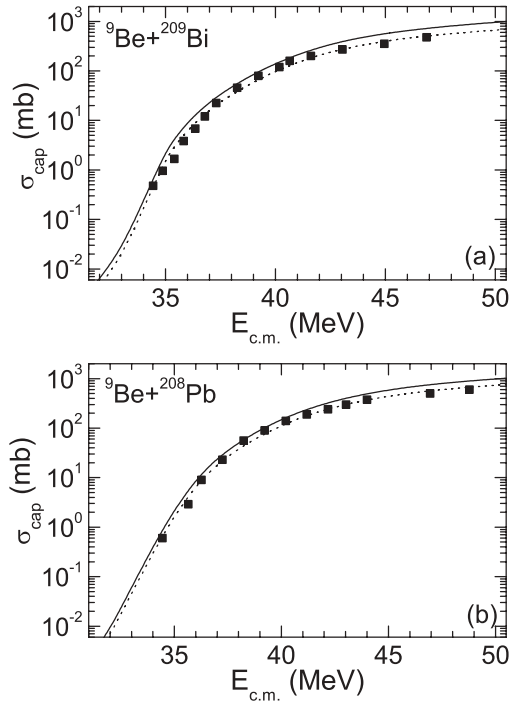


FIG. 1. The calculated capture cross sections vs $E_{c.m.}$ for the reactions ${}^9\text{Be} + {}^{209}\text{Bi}$ and ${}^9\text{Be} + {}^{208}\text{Pb}$ (solid lines). The experimental data (squares) are from Refs. [21,22]. The calculated capture cross sections normalized by factors 0.7 and 0.75 for the reactions ${}^9\text{Be} + {}^{209}\text{Bi}$ and ${}^9\text{Be} + {}^{208}\text{Pb}$, respectively, are presented by dotted lines.

transfer. Since after the transfer the mass numbers, the isotopic composition, and the deformation parameters of the interacting nuclei [and, correspondingly, the height $V_b = V(R_b)$ and shape of the Coulomb barrier] are changed, one can expect an enhancement or suppression of the capture. When the isotopic dependence of the nucleus-nucleus interaction potential is weak and the deformations of the interacting nuclei after the transfer have not changed, there is no effect of the neutron transfer on the capture cross section. This scenario was verified in the description of many reactions in Ref. [11].

III. RESULTS OF CALCULATIONS

All calculated results are obtained with the same set of parameters as in Ref. [10]. We use the friction coefficient in the relative distance coordinate, which is close to that calculated within the mean field approaches [16]. The absolute values of the quadrupole deformation parameters β_2 of even-even deformed nuclei are taken from Ref. [17]. For the nuclei deformed in the ground state, the β_2 in the first excited collective state is similar to the β_2 in the ground state. For the quadrupole deformation parameter of an odd nucleus, we choose the maximal value of the deformation parameters of neighboring even-even nuclei. For the double magic and neighboring nuclei, in the ground state we set $\beta_2 = 0$. There are uncertainties in the definition of the values of β_2 in light-mass nuclei. However, these uncertainties weakly influence the capture cross sections in the asymmetric reactions treated. In the calculations for light nuclei we use β_2 from Ref. [18].

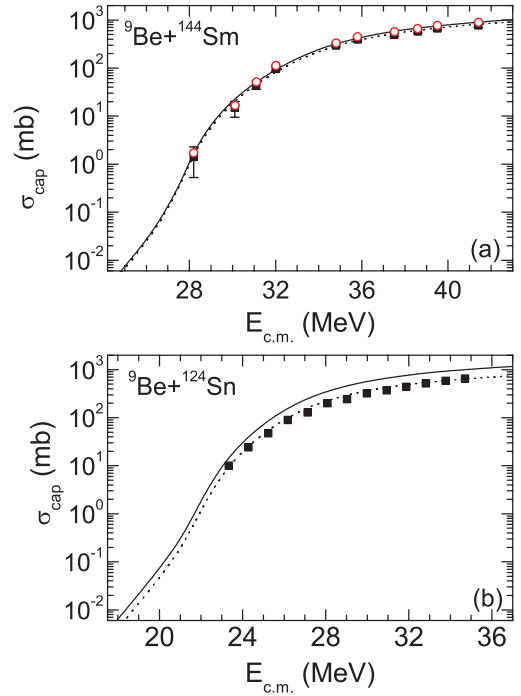


FIG. 2. (Color online) The calculated capture cross sections vs $E_{c.m.}$ for the reactions ${}^9\text{Be} + {}^{144}\text{Sm}$ and ${}^9\text{Be} + {}^{124}\text{Sn}$ (solid lines). The experimental data (squares) are from Refs. [23,24]. The experimental total fusion data [23] for the ${}^9\text{Be} + {}^{144}\text{Sm}$ reaction are shown by open circles. The calculated capture cross sections normalized by factors 0.9 and 0.64 for the reactions ${}^9\text{Be} + {}^{144}\text{Sm}$ and ${}^9\text{Be} + {}^{124}\text{Sn}$, respectively, are presented by dotted lines.

A. Breakup probabilities

In Figs. 1–13 we compare the calculated σ_c^{th} capture cross sections with the experimental $\sigma_{\text{fus}}^{\text{exp}}$ complete and total fusion cross sections in the reactions induced by projectiles ${}^9\text{Be}$, ${}^{10,11}\text{B}$, ${}^{6,7,9}\text{Li}$, and ${}^{4,6,8}\text{He}$ [19–40]. The difference between the capture cross section and the complete fusion cross section can be ascribed to the breakup effect. By comparing σ_c^{th} and $\sigma_{\text{fus}}^{\text{exp}}$, one can estimate the breakup probability

$$P_{\text{BU}} = 1 - \sigma_{\text{fus}}^{\text{exp}} / \sigma_c^{\text{th}}. \quad (1)$$

If at some energy $\sigma_{\text{fus}}^{\text{exp}} > \sigma_c^{\text{th}}$, the values of σ_c^{th} were normalized so to have $P_{\text{BU}} \geq 0$ at any energy.

Note that $\sigma_{\text{fus}}^{\text{exp}} = \sigma_{\text{fus}}^{\text{noBU}} + \sigma_{\text{fus}}^{\text{BU}}$ contains the contribution from two processes: the direct fusion of the projectile with the target ($\sigma_{\text{fus}}^{\text{noBU}}$) and the breakup of the projectile followed by the fusion of the two projectile fragments with the target ($\sigma_{\text{fus}}^{\text{BU}}$). A more adequate estimate of the breakup probability would then be

$$P_{\text{BU}} = 1 - \sigma_{\text{fus}}^{\text{noBU}} / \sigma_c^{\text{th}}, \quad (2)$$

which leads to larger values of P_{BU} than the expression employed by us. However, the ratio between $\sigma_{\text{fus}}^{\text{noBU}}$ and $\sigma_{\text{fus}}^{\text{BU}}$ cannot be measured experimentally but can be estimated with the approach suggested in Refs. [41,42]. The parameters of the potential are taken to fit the height of the Coulomb barrier obtained in our calculations. The parameters of the breakup function [41] are set to describe the value of $\sigma_{\text{fus}}^{\text{exp}}$. As shown

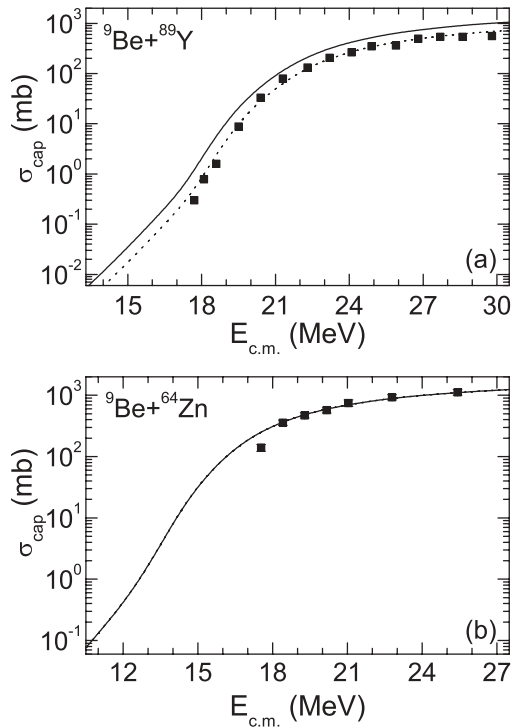


FIG. 3. The calculated capture cross sections vs $E_{\text{c.m.}}$ for the reactions ${}^9\text{Be} + {}^{89}\text{Y}$ and ${}^9\text{Be} + {}^{64}\text{Zn}$ (solid lines). The experimental data (squares) are from Refs. [25,26]. The calculated capture cross sections normalized by a factor 0.7 for the ${}^9\text{Be} + {}^{89}\text{Y}$ reaction are presented by a dotted line.

in Ref. [41] and in our calculations, in the ${}^8\text{Be} + {}^{208}\text{Pb}$ reaction the fraction of $\sigma_{\text{fus}}^{\text{BU}}$ in $\sigma_{\text{fus}}^{\text{exp}}$ does not exceed a few percent at $E_{\text{c.m.}} - V_b < 4$ MeV. This fraction rapidly increases and reaches about 12–20%, depending on the reaction, at $E_{\text{c.m.}} - V_b \approx 10$ MeV. Because we are mainly interested in the energies near and below the barrier, the estimated $\sigma_{\text{fus}}^{\text{BU}}$ does not exceed 20% of $\sigma_{\text{fus}}^{\text{exp}}$ at $E_{\text{c.m.}} - V_b < 10$ MeV. The results for P_{BU} are presented, taking $\sigma_{\text{fus}}^{\text{noBU}}$ into account, in Eq. (2).

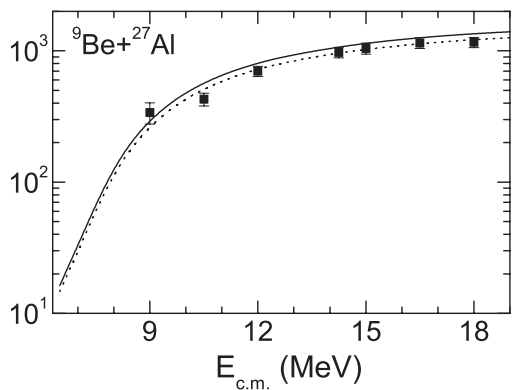


FIG. 4. The calculated capture cross sections vs $E_{\text{c.m.}}$ for the reaction ${}^9\text{Be} + {}^{27}\text{Al}$ (solid line). The experimental data (squares) are from Ref. [27]. The calculated capture cross sections normalized by a factor 0.9 for the ${}^9\text{Be} + {}^{27}\text{Al}$ reaction are presented by a dotted line.

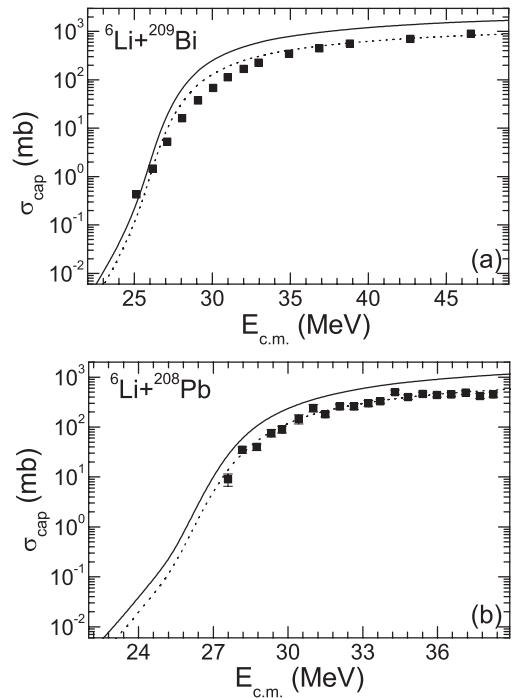


FIG. 5. The calculated capture cross sections vs $E_{\text{c.m.}}$ for the reactions ${}^6\text{Li} + {}^{209}\text{Bi}$ and ${}^6\text{Li} + {}^{208}\text{Pb}$ (solid lines). The experimental data (squares) are from Refs. [30,31]. The calculated capture cross sections normalized by factors 0.52 and 0.5 for the reactions ${}^6\text{Li} + {}^{209}\text{Bi}$ and ${}^6\text{Li} + {}^{208}\text{Pb}$, respectively, are presented by dotted lines.

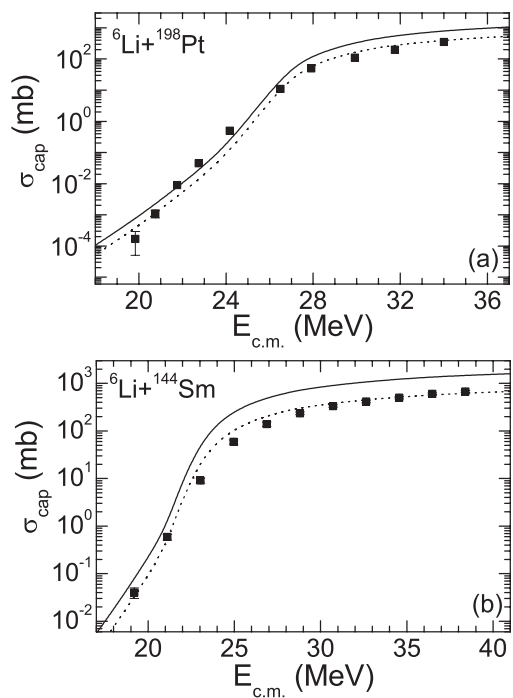


FIG. 6. The calculated capture cross sections vs $E_{\text{c.m.}}$ for the reactions ${}^6\text{Li} + {}^{198}\text{Pt}$ and ${}^6\text{Li} + {}^{144}\text{Sm}$ (solid lines). The experimental data (squares) are from Refs. [32,33]. The calculated capture cross sections normalized by factors 0.5 and 0.42 for the reactions ${}^6\text{Li} + {}^{198}\text{Pt}$ and ${}^6\text{Li} + {}^{144}\text{Sm}$, respectively, are presented by dotted lines.

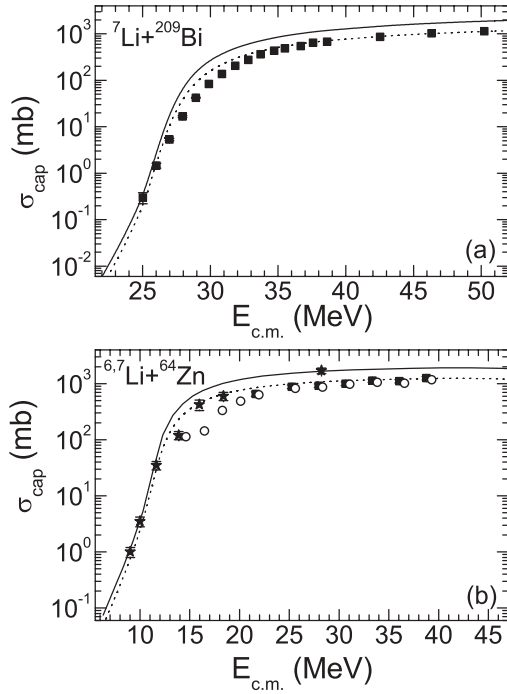


FIG. 7. The calculated capture cross sections vs $E_{c.m.}$ for the reactions ${}^7\text{Li} + {}^{209}\text{Bi}$ and ${}^7\text{Li} + {}^{64}\text{Zn}$ (solid lines). The calculated results for the reactions ${}^{6,7}\text{Li} + {}^{64}\text{Zn}$ almost coincide. The experimental data (squares) are from Refs. [26,30]. The experimental data for the reactions ${}^7\text{Li} + {}^{64}\text{Zn}$ (squares) and ${}^6\text{Li} + {}^{64}\text{Zn}$ (circles and stars) are from Refs. [26,34]. The calculated capture cross sections normalized by factors 0.6 and 0.65 for the reactions ${}^7\text{Li} + {}^{209}\text{Bi}$ and ${}^7\text{Li} + {}^{64}\text{Zn}$, respectively, are presented by dotted lines.

As seen in Figs. 14 and 15, at energies above the Coulomb barriers the values of P_{BU} vary from 0 to 84%. In the reactions ${}^9\text{Be} + {}^{144}\text{Sm}$, ${}^{208}\text{Pb}$, ${}^{209}\text{Bi}$, the value of P_{BU} increases with charge number of the target at $E_{c.m.} - V_b > 3$ MeV. This was also noted in Ref. [9]. However, the reactions ${}^9\text{Be} + {}^{89}\text{Y}$, ${}^{124}\text{Sn}$ are out of this systematics. In the reactions ${}^6\text{Li} + {}^{144}\text{Sm}$, ${}^{198}\text{Pt}$, ${}^{209}\text{Bi}$, the value of P_{BU} decreases with increasing charge number of the target at $E_{c.m.} - V_b > 3$ MeV. While in the reactions ${}^9\text{Be} + {}^{89}\text{Y}$, ${}^{144}\text{Sm}$, ${}^{208}\text{Pb}$, ${}^{209}\text{Bi}$, the value of P_{BU} has a minimum at $E_{c.m.} - V_b \approx 0$ and a maximum at $E_{c.m.} - V_b \approx -(1-3)$ MeV, in the ${}^9\text{Be} + {}^{124}\text{Sn}$ reaction the value of P_{BU} steadily decreases with energy. In the reactions ${}^6\text{Li} + {}^{144}\text{Sm}$, ${}^{198}\text{Pt}$, ${}^{209}\text{Bi}$; ${}^7\text{Li} + {}^{208}\text{Pb}$, ${}^{209}\text{Bi}$; and ${}^9\text{Li} + {}^{208}\text{Pb}$ there is maximum of P_{BU} at $E_{c.m.} - V_b \approx -(0-1)$ MeV. However, in the reactions ${}^6\text{Li} + {}^{208}\text{Pb}$ and ${}^7\text{Li} + {}^{165}\text{Ho}$ P_{BU} has a minima $E_{c.m.} - V_b \approx 2$ MeV and no maxima at $E_{c.m.} - V_b \approx 0$. For ${}^9\text{Be}$, the breakup threshold is slightly larger than for ${}^6\text{Li}$. Therefore, we cannot explain a larger breakup probability at smaller $E_{c.m.} - V_b$ in the case of ${}^9\text{Be}$.

In Figs. 1–13 we also show the calculated capture cross sections normalized by some factors to obtain rather good agreement between the experimental and theoretical results. These average normalization factors are 0.7, 0.75, 0.9, 0.64, 0.7, 1, and 0.9 for the reactions ${}^9\text{Be} + {}^{209}\text{Bi}$, ${}^{208}\text{Pb}$, ${}^{144}\text{Sm}$, ${}^{124}\text{Sn}$, ${}^{89}\text{Y}$, ${}^{64}\text{Zn}$, ${}^{27}\text{Al}$, respectively; 0.52, 0.5, 0.5, 0.42, and

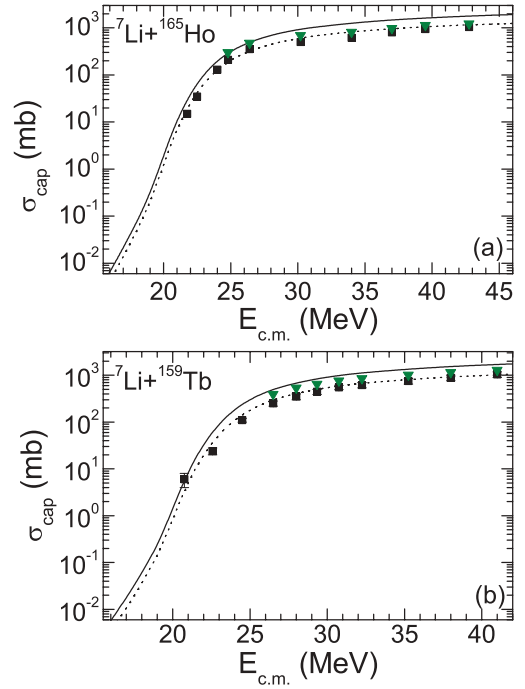


FIG. 8. (Color online) The calculated capture cross sections vs $E_{c.m.}$ for the reactions ${}^7\text{Li} + {}^{165}\text{Ho}$ and ${}^7\text{Li} + {}^{159}\text{Tb}$ (solid lines). The experimental data (squares) are from Refs. [20,35]. The experimental total fusion data [20,35] are shown by the solid triangles. The calculated capture cross sections normalized by factors 0.65 and 0.6 for the reactions ${}^7\text{Li} + {}^{165}\text{Ho}$ and ${}^7\text{Li} + {}^{159}\text{Tb}$, respectively, are presented by dotted lines.

0.65 for the reactions ${}^6\text{Li} + {}^{209}\text{Bi}$, ${}^{208}\text{Pb}$, ${}^{198}\text{Pt}$, ${}^{144}\text{Sm}$, ${}^{64}\text{Zn}$, respectively; and 0.6, 0.7, 0.65, 0.6, 0.65, and 0.75 for the reactions ${}^7\text{Li} + {}^{209}\text{Bi}$, ${}^{197}\text{Au}$, ${}^{165}\text{Ho}$, ${}^{159}\text{Tb}$, ${}^{64}\text{Zn}$, ${}^{27}\text{Al}$, respectively. For the reactions ${}^9\text{Li} + {}^{208}\text{Pb}$ (Fig. 10), ${}^6\text{He} + {}^{209}\text{Bi}$ (Fig. 11), ${}^6\text{He} + {}^{64}\text{Zn}$ (Fig. 11), ${}^6\text{He} + {}^{197}\text{Au}$ (Fig. 12), ${}^8\text{He} + {}^{197}\text{Au}$ (Fig. 12), ${}^{11}\text{B} + {}^{209}\text{Bi}$ (Fig. 13), and ${}^{11}\text{B} + {}^{159}\text{Tb}$ (Fig. 13), a satisfactory agreement between experimental fusion data and capture cross sections can be reached with average normalization factors 0.6, 0.68, 0.4, 0.8, 0.7, 0.82, and 0.95, respectively. Note that these average normalization factors do not depend on $E_{c.m.}$. With the ${}^9\text{Be}$ projectile we obtain the complete fusion suppressions similar to those reported in Refs. [6,9]. For lighter targets, when the Coulomb breakup becomes weaker, one expects that the suppression of complete fusion becomes smaller than for heavy targets.

An expected behavior for complete fusion suppression is that fusion probability increases with decreasing Z_T . However, one can observe deviations from this rule. In the reactions ${}^9\text{Be} + {}^{124}\text{Sn}$, ${}^{89}\text{Y}$ the data show more complete fusion suppression (30–36%). For the reactions induced by a ${}^6\text{Li}$ projectile, one can see that the fusion suppression is nearly independent of Z_T . The replacement of ${}^7\text{Li}$ by ${}^6\text{Li}$ in the reactions in Fig. 9 almost does not change the experimental [28,29] and calculated data. The Coulomb fields for very light systems ${}^9\text{Be} + {}^{27}\text{Al}$, and ${}^6\text{He}$, ${}^7\text{Li} + {}^{64}\text{Zn}$ are not strong enough to produce an appreciable breakup. It is not realistic that the fusion suppression in the ${}^9\text{Be} + {}^{64}\text{Zn}$ reaction is smaller than

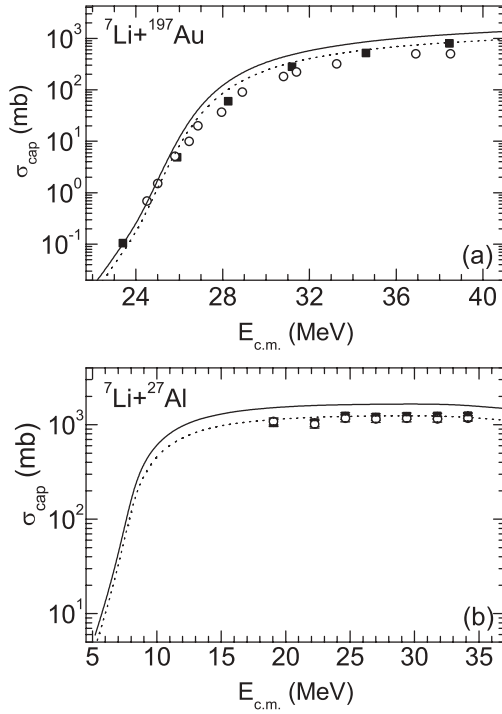


FIG. 9. The calculated capture cross sections vs $E_{c.m.}$ for the reactions ${}^7\text{Li} + {}^{197}\text{Au}$ and ${}^7\text{Li} + {}^{27}\text{Al}$ (solid lines). The experimental data (squares) are from Refs. [28,29]. The calculated capture cross sections normalized by factors 0.7 and 0.75 for the reactions ${}^7\text{Li} + {}^{197}\text{Au}$ and ${}^7\text{Li} + {}^{27}\text{Al}$, respectively, are presented by dotted lines.

the one in the ${}^9\text{Be} + {}^{27}\text{Al}$ reaction or the suppressions of fusion coincide in the reactions ${}^{4,6}\text{He} + {}^{64}\text{Zn}$ (Fig. 11) with stable and exotic projectiles. Note that the experimental data for the reactions ${}^{6,7}\text{Li} + {}^{27}\text{Al}$, ${}^{64}\text{Zn}$ and ${}^9\text{Be} + {}^{27}\text{Al}$, ${}^{64,70}\text{Zn}$ are for the total fusion. In general, the total fusion does not seem to be affected by breakup [6,9].

So, there is a lack of a systematic behavior of the complete fusion suppression for the systems treated. The possible explanation is that there are probably some problems with the data analysis, which were earlier noted in Refs. [6,9] from the point of view of a universal fusion function representation. It could be also that at energies near the Coulomb barrier the characteristic time of the breakup is larger than the characteristic time of the capture process and influences the complete fusion. For the reactions ${}^{6,7}\text{Li} + {}^{208}\text{Pb}$, the characteristic times of the prompt and delayed breakup were studied recently in Ref. [43].

The large positive Q_{2n} value in the ${}^9\text{Li} + {}^{208}\text{Pb}$ reaction [40] gives the possibility of a two-neutron transfer before the capture. However, the capture cross sections calculated with and without neutron transfer are very close to each other because the effect of neutron transfer is rather weak in asymmetric reactions [10,11]. The calculated capture cross sections normalized by a factor of 0.6 are shown by the dotted line in the lower part of Fig. 10. In the upper part of Fig. 10, the predicted capture cross sections for the reaction ${}^{11}\text{Li} + {}^{208}\text{Pb}$ are shown.

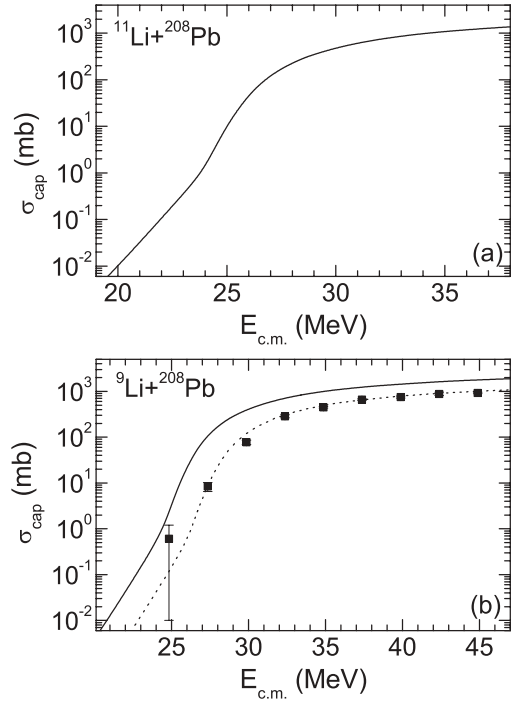


FIG. 10. The calculated capture cross sections vs $E_{c.m.}$ for the reactions ${}^{11}\text{Li} + {}^{208}\text{Pb}$ and ${}^9\text{Li} + {}^{208}\text{Pb}$ (solid lines). The experimental data (squares) are from Ref. [40]. The calculated capture cross sections normalized by a factor 0.6 for the ${}^9\text{Li} + {}^{208}\text{Pb}$ reaction are presented by a dotted line.

B. Quasielastic backscattering tool for search of breakup process in reactions with weakly bound projectiles

The lack of clear systematic behavior of the complete fusion suppression as a function of the target charge requires new additional experimental and theoretical studies. Quasielastic backscattering has been used [44–47] as an alternative to investigate fusion (capture) barrier distributions, since this process is complementary to fusion. Since the quasielastic experiment is usually not as complex as the capture (fusion) and breakup measurements, they are well suited to survey the breakup probability. There is a direct relationship among the capture, the quasielastic scattering, and the breakup processes, since any loss from the quasielastic and breakup channel contributes directly to capture (the conservation of the reaction flux):

$$P_{qe}(E_{c.m.}, J) + P_{cap}(E_{c.m.}, J) + P_{BU}(E_{c.m.}, J) = 1, \quad (3)$$

where P_{qe} is the reflection quasielastic probability, P_{BU} is the breakup (reflection) probability, and P_{cap} is the capture (transmission) probability. The quasielastic scattering is the sum of all direct reactions, which include elastic, inelastic, and transfer processes. Equation (3) can be rewritten as

$$\frac{P_{qe}(E_{c.m.}, J)}{1 - P_{BU}(E_{c.m.}, J)} + \frac{P_{cap}(E_{c.m.}, J)}{1 - P_{BU}(E_{c.m.}, J)} = P_{qe}^{nBU}(E_{c.m.}, J) + P_{cap}^{nBU}(E_{c.m.}, J) = 1, \quad (4)$$

where

$$P_{qe}^{nBU}(E_{c.m.}, J) = \frac{P_{qe}(E_{c.m.}, J)}{1 - P_{BU}(E_{c.m.}, J)}$$

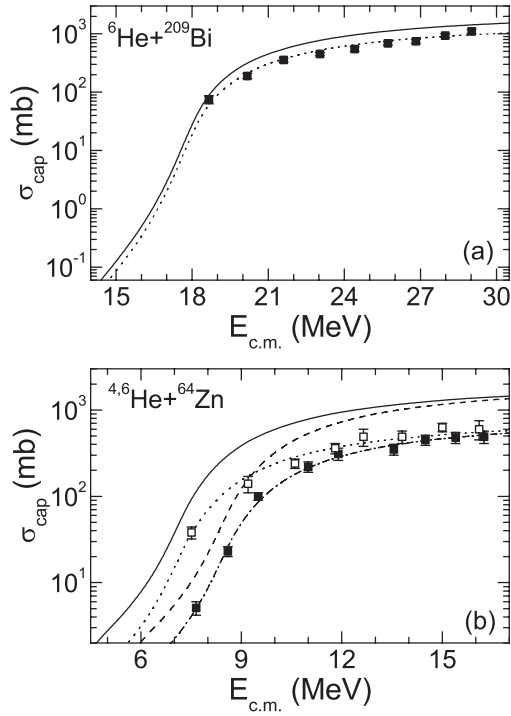


FIG. 11. The calculated capture cross sections vs $E_{\text{c.m.}}$ for the indicated reactions ${}^6\text{He} + {}^{209}\text{Bi}$ (solid line), ${}^6\text{He} + {}^{64}\text{Zn}$ (solid line), and ${}^4\text{He} + {}^{64}\text{Zn}$ (dashed line). The experimental data for the reactions ${}^4\text{He} + {}^{64}\text{Zn}$ (solid squares) and ${}^6\text{He} + {}^{64}\text{Zn}$ (open squares) are from Refs. [36,37]. The calculated capture cross sections normalized by factors 0.68, 0.4, and 0.4 for the reactions ${}^6\text{He} + {}^{209}\text{Bi}$ (dotted line), ${}^6\text{He} + {}^{64}\text{Zn}$ (dotted line), and ${}^4\text{He} + {}^{64}\text{Zn}$ (dash-dotted line), respectively, are shown.

and

$$P_{\text{cap}}^{\text{nBU}}(E_{\text{c.m.}}, J) = \frac{P_{\text{cap}}(E_{\text{c.m.}}, J)}{1 - P_{\text{BU}}(E_{\text{c.m.}}, J)}$$

are the quasielastic and capture probabilities, respectively, in the absence of the breakup process. From these expressions we obtain the useful formulas

$$\begin{aligned} \frac{P_{\text{qe}}(E_{\text{c.m.}}, J)}{P_{\text{cap}}(E_{\text{c.m.}}, J)} &= \frac{P_{\text{qe}}^{\text{nBU}}(E_{\text{c.m.}}, J)}{P_{\text{cap}}^{\text{nBU}}(E_{\text{c.m.}}, J)} \\ &= \frac{P_{\text{qe}}^{\text{nBU}}(E_{\text{c.m.}}, J)}{1 - P_{\text{qe}}^{\text{nBU}}(E_{\text{c.m.}}, J)} = a. \end{aligned} \quad (5)$$

Using Eqs. (3) and (5), we obtain the relationship between breakup and quasielastic processes:

$$\begin{aligned} P_{\text{BU}}(E_{\text{c.m.}}, J) &= 1 - [P_{\text{qe}}(E_{\text{c.m.}}, J) + P_{\text{cap}}(E_{\text{c.m.}}, J)] \\ &= 1 - P_{\text{qe}}(E_{\text{c.m.}}, J)[1 + 1/a] \\ &= 1 - P_{\text{qe}}(E_{\text{c.m.}}, J)/P_{\text{qe}}^{\text{nBU}}(E_{\text{c.m.}}, J). \end{aligned} \quad (6)$$

The last equation is one of important results of the present paper. Analogously one can find other expression

$$P_{\text{BU}}(E_{\text{c.m.}}, J) = 1 - P_{\text{cap}}(E_{\text{c.m.}}, J)/P_{\text{cap}}^{\text{nBU}}(E_{\text{c.m.}}, J), \quad (7)$$

which relates the breakup and capture processes.

The reflection quasielastic probability

$$P_{\text{qe}}(E_{\text{c.m.}}, J = 0) = d\sigma_{\text{qe}}/d\sigma_{\text{Ru}} \quad (8)$$

for bombarding energy $E_{\text{c.m.}}$ and angular momentum $J = 0$ is given by the ratio of the quasielastic differential cross section σ_{qe} and Rutherford differential cross section σ_{Ru} at 180 degrees [44–48]. Employing Eqs. (6), (8), and the experimental quasielastic backscattering data with strongly and weakly bound isotope projectiles and the same compound nucleus, one can extract the breakup probability of the exotic nucleus. For example, using Eq. (6) at $J = 0$ and the experimental $P_{\text{qe}}^{\text{nBU}}[{}^4\text{He} + {}^{208}\text{Pb}]$ of the ${}^4\text{He} + {}^{208}\text{Pb}$ reaction with strongly bound nuclei (without breakup) and $P_{\text{qe}}[{}^6\text{He} + {}^{206}\text{Pb}]$ of the ${}^6\text{He} + {}^{206}\text{Pb}$ reaction with weakly bound projectile (with breakup), and taking into consideration $V_b({}^4\text{He} + {}^{208}\text{Pb}) \approx V_b({}^6\text{He} + {}^{206}\text{Pb})$ for the very asymmetric systems, one can extract the breakup probability of ${}^6\text{He}$:

$$\begin{aligned} P_{\text{BU}}(E_{\text{c.m.}}, J = 0) &= 1 - \frac{P_{\text{qe}}(E_{\text{c.m.}}, J = 0)[{}^6\text{He} + {}^{206}\text{Pb}]}{P_{\text{qe}}^{\text{nBU}}(E_{\text{c.m.}}, J = 0)[{}^4\text{He} + {}^{208}\text{Pb}]}. \end{aligned} \quad (9)$$

By comparing the experimental quasielastic backscattering cross sections in the presence and absence of breakup data

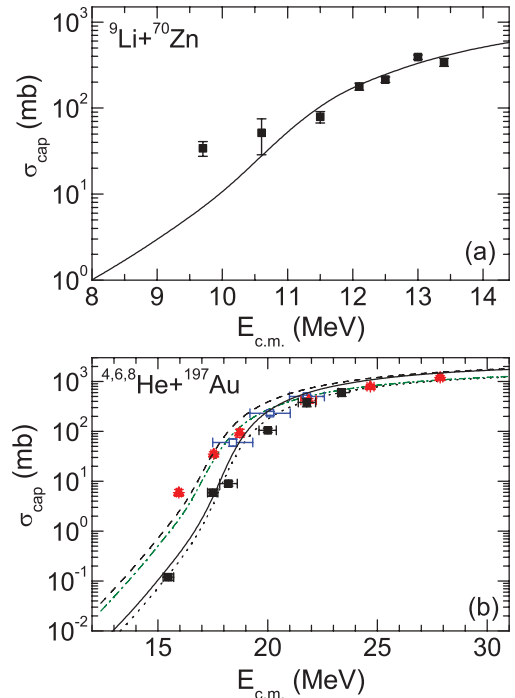


FIG. 12. (Color online) The calculated capture cross sections vs $E_{\text{c.m.}}$ for the reactions ${}^9\text{Li} + {}^{70}\text{Zn}$ (solid line), ${}^4\text{He} + {}^{197}\text{Au}$ (solid lines), and ${}^8\text{He} + {}^{197}\text{Au}$ (dashed line). The results for the reactions ${}^{4,6,8}\text{He} + {}^{197}\text{Au}$ almost coincide. The experimental data for the reactions with ${}^9\text{Li}$, ${}^4\text{He}$ (solid squares), ${}^6\text{He}$ (open squares), and ${}^8\text{He}$ (solid triangles) are from Refs. [38,39]. The calculated capture cross sections normalized by factors 0.8 and 0.6 for the reactions ${}^{4,6}\text{He} + {}^{197}\text{Au}$ (dotted lines) and ${}^8\text{He} + {}^{197}\text{Au}$ (dash-dotted line), respectively, are shown.

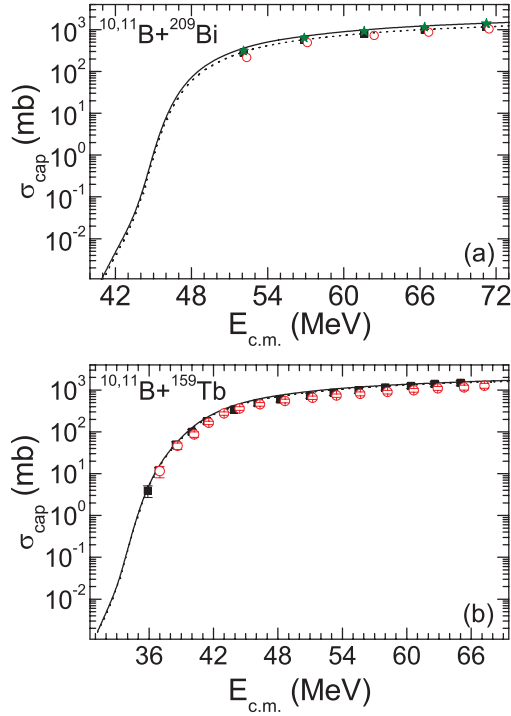


FIG. 13. (Color online) The calculated capture cross sections vs $E_{\text{c.m.}}$ for the reactions $^{10,11}\text{B} + ^{209}\text{Bi}$ and $^{10,11}\text{B} + ^{159}\text{Tb}$ (solid lines). The experimental data [19,20] for the reactions $^{10}\text{B} + ^{159}\text{Tb}$, ^{209}Bi and $^{11}\text{B} + ^{159}\text{Tb}$, ^{209}Bi are marked by circles and squares, respectively. The experimental total fusion data [19] are shown by the solid stars. The calculated capture cross sections normalized by factors 0.82 and 0.95 for the reactions $^{11}\text{B} + ^{209}\text{Bi}$ and $^{11}\text{B} + ^{159}\text{Tb}$, respectively, are presented by dotted lines.

in the reaction pairs $^6\text{He} + ^{68}\text{Zn}$ and $^4\text{He} + ^{70}\text{Zn}$, $^6\text{He} + ^{122}\text{Sn}$ and $^4\text{He} + ^{124}\text{Sn}$, $^6\text{He} + ^{236}\text{U}$ and $^4\text{He} + ^{238}\text{U}$, $^8\text{He} + ^{204}\text{Pb}$ and $^4\text{He} + ^{208}\text{Pb}$, $^9\text{Be} + ^{208}\text{Pb}$ and $^{10}\text{Be} + ^{207}\text{Pb}$, $^{11}\text{Be} + ^{206}\text{Pb}$ and $^{10}\text{Be} + ^{207}\text{Pb}$, $^8\text{B} + ^{208}\text{Pb}$ and $^{10}\text{B} + ^{206}\text{Pb}$, $^8\text{B} + ^{207}\text{Pb}$ and $^{11}\text{B} + ^{204}\text{Pb}$, $^9\text{B} + ^{208}\text{Pb}$ and $^{11}\text{B} + ^{206}\text{Pb}$, $^{15}\text{C} + ^{207}\text{Pb}$ and $^{14}\text{C} + ^{208}\text{Pb}$, and $^{17}\text{F} + ^{206}\text{Pb}$ and $^{19}\text{F} + ^{208}\text{Pb}$, leading to the same corresponding compound nuclei, one can analyze the role of the breakup channels in the reactions with the light weakly bound projectiles $^6,8\text{He}$, $^9,11\text{Be}$, $^8,9\text{B}$, ^{15}C , and ^{17}F at near and below barrier energies. One concludes that the quasielastic technique could be a very important tool in breakup research. We propose to extract the breakup probability directly from the quasielastic cross sections of systems mentioned above.

IV. SUMMARY

Comparing the calculated capture cross sections in the absence of breakup data and experimental complete fusion data, we analyzed the role of the breakup channels in the reactions with the light projectiles ^9Be , $^{6,7,9}\text{Li}$, and $^6,8\text{He}$ at near-barrier energies. Within the quantum diffusion approach the neutron transfer and deformation effects were taken into account. By analyzing the extracted breakup probabilities,

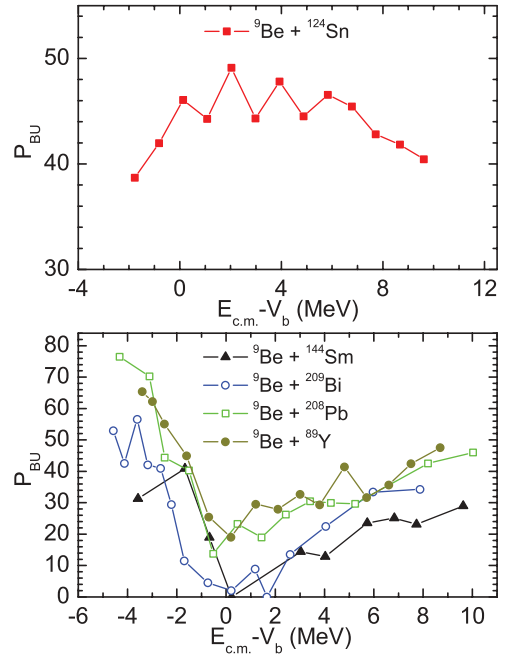


FIG. 14. (Color online) The dependence of the extracted breakup probability P_{BU} vs $E_{\text{c.m.}} - V_b$ for the indicated reactions with ^9Be projectiles in %. Formula (2) was used.

we showed that there are no systematic trends of breakup in the reactions studied. Moreover, for some system with larger (smaller) Z_T we found the contribution of breakup to be smaller (larger). Almost for all reactions considered we obtained a satisfactory agreement between calculated capture cross section and experimental fusion data, if the calculated

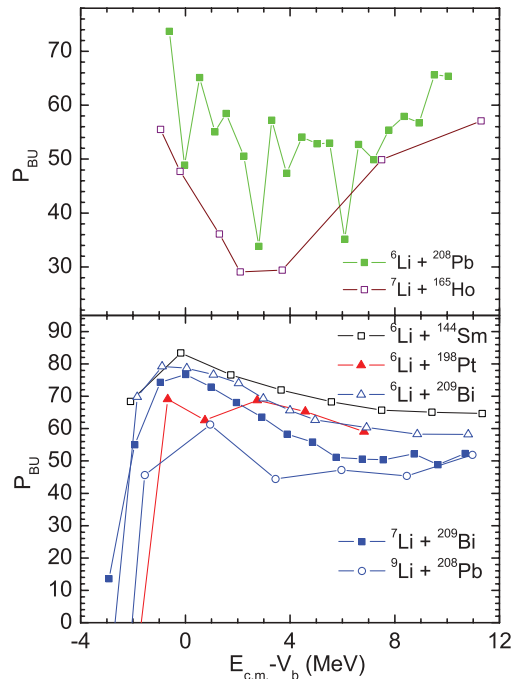


FIG. 15. (Color online) The same as in Fig. 14, but for the indicated reactions with $^{6,7,9}\text{Li}$ projectiles.

capture cross section or the experimental fusion data are renormalized by some average factor that does not depend on the bombarding energy. Note that our conclusions coincide with those of Refs. [6,9], where the universal fusion function formalism was applied for the analysis of experimental data. One needs to measure directly the breakup process in different systems, especially light ones, to understand the role of the Coulomb breakup in the complete fusion process. The other important subject to be investigated both experimentally and theoretically is the characteristic time of the breakup. The first steps in these directions were done in Refs. [7,43,49].

As shown, one no needs to measure directly the breakup process in different systems, especially light ones, to understand the role of the breakup in the capture (complete fusion) process. By employing the experimental quasielastic

backscattering data with weakly and strongly bound isotopes of light nucleus and Eq. (6), the dependence of breakup probability on $E_{c.m.}$ can be extracted for the systems suggested. By analyzing the extracted breakup probabilities, one can indirectly study the trends of breakup in the different reactions at energies near and below Coulomb barrier.

ACKNOWLEDGMENTS

We thank P. R. S. Gomes for very fruitful discussions and useful suggestions. This work was supported by DFG, NSFC, and RFBR. The IN2P3(France)-JINR(Dubna) and Polish - JINR(Dubna) Cooperation Programmes are gratefully acknowledged.

-
- [1] C. A. Bertulani, *EPJ Web Conf.* **17**, 15001 (2011); P. R. S. Gomes, J. Lubian, and L. F. Canto, *ibid.* **17**, 11003 (2011); P. R. S. Gomes *et al.*, *ibid.* (to be published).
- [2] L. F. Canto, P. R. S. Gomes, R. Donangelo, and M. S. Hussein, *Phys. Rep.* **424**, 1 (2006).
- [3] N. Keeley, R. Raabe, N. Alamanos, and J. L. Sida, *Prog. Part. Nucl. Phys.* **59**, 579 (2007).
- [4] L. F. Canto, P. R. S. Gomes, J. Lubian, L. C. Chamon, and E. Crema, *J. Phys. G* **36**, 015109 (2009).
- [5] L. F. Canto, P. R. S. Gomes, J. Lubian, L. C. Chamon, and E. Crema, *Nucl. Phys. A* **821**, 51 (2009).
- [6] P. R. S. Gomes, J. Lubian, and L. F. Canto, *Phys. Rev. C* **79**, 027606 (2009).
- [7] R. Rafiei, R. du Rietz, D. H. Luong, D. J. Hinde, M. Dasgupta, M. Evers, and A. Diaz-Torres, *Phys. Rev. C* **81**, 024601 (2010).
- [8] P. N. de Faria, R. Lichtenthaler, K. C. C. Pires, A. M. Moro, A. Lepine-Szily, V. Guimaraes, D. R. J. Mendes, A. Arazi, A. Barioni, V. Morcelle, and M. C. Morais, *Phys. Rev. C* **82**, 034602 (2010); P. Mohr, P. N. de Faria, R. Lichtenthaler, K. C. C. Pires, V. Guimaraes, A. Lepine-Szily, D. R. Mendes Jr., A. Arazi, A. Barioni, V. Morcelle, and M. C. Morais, *ibid.* **82**, 044606 (2010); A. Lepine-Szily *et al.*, *EPJ Web Conf.* (to be published).
- [9] P. R. S. Gomes, R. Linares, J. Lubian, C. C. Lopes, E. N. Cardozo, B. H. F. Pereira, and I. Padron, *Phys. Rev. C* **84**, 014615 (2011).
- [10] V. V. Sargsyan, G. G. Adamian, N. V. Antonenko, and W. Scheid, *Eur. Phys. J. A* **45**, 125 (2010); V. V. Sargsyan, G. G. Adamian, N. V. Antonenko, W. Scheid, and H. Q. Zhang, *ibid.* **47**, 38 (2011); *J. Phys.: Conf. Ser.* **282**, 012001 (2011); *EPJ Web Conf.* **17**, 04003 (2011); V. V. Sargsyan, G. G. Adamian, N. V. Antonenko, W. Scheid, C. J. Lin, and H. Q. Zhang, *Phys. Rev. C* **85**, 017603 (2012); **85**, 037602 (2012).
- [11] V. V. Sargsyan, G. G. Adamian, N. V. Antonenko, W. Scheid, and H. Q. Zhang, *Phys. Rev. C* **84**, 064614 (2011); **85**, 024616 (2012); **86**, 014602 (2012); **86**, 034614 (2012).
- [12] S. Ayik, B. Yilmaz, and D. Lacroix, *Phys. Rev. C* **81**, 034605 (2010).
- [13] A. S. Zubov, V. V. Sargsyan, G. G. Adamian, and N. V. Antonenko, *Phys. Rev. C* **84**, 044320 (2011); A. S. Zubov, V. V. Sargsyan, G. G. Adamian, N. V. Antonenko, and W. Scheid, *ibid.* **81**, 024607 (2010); **82**, 034610 (2010); R. A. Kuzyakin, V. V. Sargsyan, G. G. Adamian, N. V. Antonenko, E. E. Saperstein, and S. V. Tolokonnikov, *ibid.* **85**, 034612 (2012).
- [14] H. Hofmann, *Phys. Rep.* **284**, 137 (1997); S. Ayik, B. Yilmaz, A. Gokalp, O. Yilmaz, and N. Takigawa, *Phys. Rev. C* **71**, 054611 (2005); V. V. Sargsyan, Z. Kanokov, G. G. Adamian, and N. V. Antonenko, *Part. Nucl.* **41**, 175 (2010); G. Hupin and D. Lacroix, *Phys. Rev. C* **81**, 014609 (2010).
- [15] S. Szilner *et al.*, *Phys. Rev. C* **76**, 024604 (2007); **84**, 014325 (2011); L. Corradi *et al.*, *ibid.* **84**, 034603 (2011).
- [16] G. G. Adamian, A. K. Nasirov, N. V. Antonenko, and R. V. Jolos, *Phys. Part. Nucl.* **25**, 583 (1994); K. Washiyama, D. Lacroix, and S. Ayik, *Phys. Rev. C* **79**, 024609 (2009); S. Ayik, K. Washiyama, and D. Lacroix, *ibid.* **79**, 054606 (2009).
- [17] S. Raman, C. W. Nestor Jr., and P. Tikkanen, *At. Data Nucl. Data Tables* **78**, 1 (2001).
- [18] Y. Kanada-En'yo, H. Horiuchi, and A. Ono, *Phys. Rev. C* **52**, 628 (1995); A. Dote, H. Horiuchi, and Y. Kanada-En'yo, *ibid.* **56**, 1844 (1997).
- [19] L. R. Gasques, D. J. Hinde, M. Dasgupta, A. Mukherjee, and R. G. Thomas, *Phys. Rev. C* **79**, 034605 (2009).
- [20] A. Mukherjee *et al.*, *Phys. Lett. B* **636**, 91 (2006).
- [21] C. Signorini *et al.*, *Nucl. Phys. A* **735**, 329 (2004); M. Dasgupta, D. J. Hinde, S. L. Sheehy, and B. Bouriquet, *Phys. Rev. C* **81**, 024608 (2010).
- [22] M. Dasgupta *et al.*, *Phys. Rev. Lett.* **82**, 1395 (1999).
- [23] P. R. S. Gomes *et al.*, *Phys. Rev. C* **73**, 064606 (2006).
- [24] V. V. Parkar *et al.*, *Phys. Rev. C* **82**, 054601 (2010).
- [25] C. S. Palshetkar *et al.*, *Phys. Rev. C* **82**, 044608 (2010).
- [26] P. R. S. Gomes *et al.*, *Phys. Rev. C* **71**, 034608 (2005).
- [27] G. V. Marti *et al.*, *Phys. Rev. C* **71**, 027602 (2005).
- [28] I. Padron *et al.*, *Phys. Rev. C* **66**, 044608 (2002).
- [29] Sh. Thakur *et al.*, *EPJ Web Conf.* **17**, 16017 (2011).
- [30] M. Dasgupta *et al.*, *Phys. Rev. C* **70**, 024606 (2004).
- [31] Y. W. Wu *et al.*, *Phys. Rev. C* **68**, 044605 (2003).
- [32] A. Shrivastava *et al.*, *Phys. Rev. Lett.* **103**, 232702 (2009).
- [33] P. K. Rath *et al.*, *Phys. Rev. C* **79**, 051601(R) (2009).
- [34] D. Torresi *et al.*, *EPJ Web Conf.* **17**, 16018 (2011).
- [35] V. Tripathi, A. Navin, K. Mahata, K. Ramachandran, A. Chatterjee, and S. Kailas, *Phys. Rev. Lett.* **88**, 172701 (2002).
- [36] J. J. Kolata *et al.*, *Eur. Phys. J. A* **13**, 117 (2002).
- [37] M. Fisichella *et al.*, *EPJ Web Conf.* **17**, 16003 (2011).

- [38] W. Loveland *et al.*, *Phys. Rev. C* **74**, 064609 (2006); W. Loveland, *EPJ Web Conf.* **17**, 02003 (2011).
- [39] A. Lemasson *et al.*, *Phys. Rev. Lett.* **103**, 232701 (2009); *EPJ Web Conf.* **17**, 01003 (2011).
- [40] A. M. Vinodkumar *et al.*, *Phys. Rev. C* **80**, 054609 (2009).
- [41] A. Diaz-Torres, *J. Phys. G* **37**, 075109 (2010).
- [42] A. Diaz-Torres, *Comput. Phys. Commun.* **182**, 1100 (2011).
- [43] D. H. Luong *et al.*, *Phys. Lett. B* **695**, 105 (2011); *EPJ Web Conf.* **17**, 03002 (2011).
- [44] H. Timmers, J. R. Leigh, M. Dasgupta, D. J. Hinde, R. C. Lemmon, J. C. Mein, C. R. Morton, J. O. Newton, and N. Rowley, *Nucl. Phys. A* **584**, 190 (1995); H. Timmers *et al.*, *J. Phys. G* **23**, 1175 (1997); *Nucl. Phys. A* **633**, 421 (1998); T. J. Schuck, H. Timmers, and M. Dasgupta, *ibid.* **712**, 14 (2002).
- [45] H. Q. Zhang, F. Yang, C. Lin, Z. Liu, and Y. Hu, *Phys. Rev. C* **57**, R1047 (1998); H. Q. Zhang *et al.*, *Inter. Workshop on Nuclear Reactions and Beyond*, edited by G. M. Jin, Y. X. Luo, and F. S. Zhang (World Scientific, Singapore, 2000), p. 95; C. J. Lin *et al.*, *Nucl. Phys. A* **787**, 281c (2007); F. Yang, C. J. Lin, X. K. Wu, H. Q. Zhang, C. L. Zhang, P. Zhou, and Z. H. Liu, *Phys. Rev. C* **77**, 014601 (2008); H. M. Jia *et al.*, *ibid.* **82**, 027602 (2010).
- [46] S. Sinha, M. R. Pahlavani, R. Varma, R. K. Choudhury, B. K. Nayak, and A. Saxena, *Phys. Rev. C* **64**, 024607 (2001).
- [47] E. Piasecki *et al.*, *Phys. Rev. C* **65**, 054611 (2002); **80**, 054613 (2009); **85**, 054604 (2012); **85**, 054608 (2012).
- [48] A. A. Sonzogni, J. D. Bierman, M. P. Kelly, J. P. Lestone, J. F. Liang, and R. Vandenbosch, *Phys. Rev. C* **57**, 722 (1998); O. A. Capurro *et al.*, *ibid.* **61**, 037603 (2000); S. Santra, P. Singh, S. Kailas, Q. Chatterjee, A. Shrivasta, and K. Mahata, *ibid.* **64**, 024602 (2001); R. F. Simões *et al.*, *Phys. Lett. B* **527**, 187 (2002); D. S. Monteiro *et al.*, *Phys. Rev. C* **79**, 014601 (2009).
- [49] P. R. S. Gomes (private communication).